2014 International Conference on Unmanned Aircraft Systems (ICUAS)
May 27-30, 2014. Orlando, FL, USA

Morphological Filtering and Target Tracking for Vision-based UAS Sense and Avoid

Giancarmine Fasano, Domenico Accardo, Anna Elena Tirri, Antonio Moccia, *Senior Member, IEEE*, and Ettore De Lellis

Abstract— **This paper presents a customized detection and tracking algorithm for vision-based non cooperative UAS sense and avoid. Obstacle detection and tentative tracking for track confirmation are based on top-hat and bottom-hat morphological filtering, local image analysis for a limited set of regions of interest, and a multi-frame processing in stabilized coordinates. Once firm tracking is achieved, template matching and state estimation based on Kalman filtering are used to track the intruder aircraft and estimate its angular position and velocity. The developed technique has been tested using flight data gathered in a sense and avoid research project carried out by the Italian Aerospace Research Center and the Department of Industrial Engineering of the university of Naples "Federico II". Performance evaluated in two near collision geometries allows estimating algorithm robustness in terms of sensitivity on weather and illumination conditions, detection range and false alarm rate, and overall tracking accuracy.**

I. Introduction

The access of Unmanned Aircraft Systems (UAS) to civil airspace is a key issue to increase the capabilities and the level of awareness for several human activities such as homeland security, disaster monitoring and mitigation, and general surveillance applications. Significant efforts are being carried out to this aim, with the first FAA UAS Integration Roadmap [1] representing the most recent result of regulatory activities in the United States. Within this framework, the different UAS classes must be taken into account, as they vary in size, speeds, maneuverability, environmental conditions and airspace classes in which they are expected to fly.

In general, sense and avoid is one of the key integration challenges, and the surveillance function for separation assurance and collision avoidance can be performed by two fundamental methods: cooperative instruments, wherein an aircraft is equipped with a transponder to interrogate and/or broadcast information, and non-cooperative sensors, which are able to detect targets autonomously.

Among cooperative systems, it can be foreseen that ADS-B (Automatic Dependant Surveillance - Broadcast) will play a key role for the integration of UAS into civil airspace, and the use of ADS-B as primary safety system seems to be a promising opportunity also for small UAS with limited budgets in terms of power, size, mass, and cost, for which separation assurance and collision avoidance represent a challenging problem [2].

Within non cooperative architectures, which can also ensure avoidance of non equipped aircraft, radars and electro-optical (EO) sensors are the main technologies under analysis. In particular, radars represent a suitable option to provide the required situational awareness in the case of larger UAS platforms, which have to attain a reliable full autonomy from ground, while EO sensors are a viable solution for smaller platforms with limited budgets. In fact, sensing solutions proposed in literature range from standalone EO sensors [3-6] to multi-sensor radar/EO systems [7] and integrated architectures comprising radars, optical sensors, and cooperative systems [8].

In view of medium/large UAS, within the research project named TECVOL the Italian Aerospace Research Center (CIRA) and the University of Naples "Federico II" developed a prototype Sense and Avoid system which relies on an integrated radar/EO configuration [7]. Recent papers describe flight results regarding radar-based intruder detection and tracking [9], radar/EO fusion [10], and autonomous non-cooperative collision avoidance [11].

This paper results instead from a different and more recent research effort focused on smaller UAS and aimed at evaluating standalone EO sense and avoid capabilities [12]. While this research can effectively take advantage from the experimental data base gathered in TECVOL, it is important to underline its originality with respect to previous work relevant to multi-sensor-based systems.

In particular, the paper describes a detection and tracking algorithm which was developed to detect and track intruder approaching from above the horizon. Detection of intruders hidden in ground clutter is a different problem [4], and it likely requires multi-frame image processing approaches with camera frame rate as a key parameter.

Several different approaches have been considered in literature for vision-based detection of flying obstacles, such as:

- optical flow [3];

- morphological filtering followed by track-before-detect temporal filtering [4]. Hidden Markov Models have been shown to be the most effective multi-temporal technique, on the basis of flight data;

G. Fasano, D. Accardo, A.E. Tirri, and A. Moccia are with the Department of Industrial Engineering, University of Naples "Federico II", P.le Tecchio 80, 80125 Napoli, Italy (e-mails: giancarmine.fasano@unina.it, domenico.accardo@unina.it, annaelena.tirri@unina.it, antonio.moccia@unina.it).

E. De Lellis is with the On-Board Systems And ATM Information Technologies Department, Italian Aerospace Research Center, via Maiorise, 81043 Capua CE, Italy (e-mail: e.delellis@cira.it).

- morphological filtering augmented with a trained classifier [5]. Ground-based aircraft data demonstrated in this work a very large detection range. Of course, this type of methods has a strong dependency on the training data set;

- adaptive thresholding and local image analysis [6].

This work presents an original algorithm for vision-based aircraft detection and tracking, where morphological filters are augmented by local image analyses, a multi-frame logic in stabilized coordinates is used to confirm intruder detection, and firm tracking is based on template matching and Kalman filtering-based state estimation. The latter algorithm allows estimating intruder angular motion which in general is very important for collision threat estimation.

The paper is organized as follows. First, the developed algorithm is described in detail. Then, after a very brief overview of flight system setup and testing architecture, results from off-line simulations based on flight data are described. Performance in two near collision encounters, relevant to flight tests in different weather and illumination conditions, is finally discussed in terms of detection range, robustness to false detections, and overall tracking accuracy.

II. ARCHITECTURE AND ALGORITHMS

The developed algorithm is in general aimed at multi-target detection and tracking. However, it is not aimed at tracking closely spaced targets, which are unlikely to be found in civil sense and avoid scenarios. The proposed approach is a combination of low level image processing techniques and high level state estimation algorithms. It combines electro-optical data with own-ship navigation system measurements, and comprises two steps:

1. target detection and tentative tracking, which is aimed at isolating measurements which can be associated with good confidence to a real intruder aircraft;

2. firm tracking, which is aimed at a reliable estimation of intruder angular position (in spite of temporary missed detections) and velocity, which is an important variable for estimating collision threat.

The processing steps are described in the two sub-sections below. Then, considerations and the processing strategy relevant to algorithm tuning are provided.

A. Detection and tentative tracking: morphological filtering and local image analysis

Obstacle detection is based on morphological filtering operations. Morphological techniques represent a commonly adopted tool in image processing [13] and can be effectively used to detect small dim targets against non homogeneous background. They require the definition of a "structuring element" that allows controlling size and shape of the features to be highlighted in an image. Classical morphological operations used to highlight and detect small image features comprise close-minus-open (CMO) processing, bottom hat (BH), and top hat (TH) filtering. In particular, BH filters are useful to detect features that are darker than the background, TH processing extracts brighter features than the background, while CMO algorithms can be used to detect both darker and brighter pixels. Recent approaches comprise adaptive contour-based morphology (ACBM) [14] where properties of the target, such as the continuity of variation of pixel intensities within the target region, are taken into account.

In the considered implementation, the first operation that is carried out is to remove the below the horizon part of the image, so that all the subsequent calculations are carried out only in the sky region. Due to the relatively narrow camera field of view (FOV), horizon can be considered (at a first level of approximation) as a line segment, and its extreme points within the image can be calculated by considering height above ground, roll and pitch angles, and the alignment matrix that converts from the aircraft body reference frame (BRF) to the camera reference frame. This alignment matrix can be estimated off line by a proper alignment procedure [15], while the other equations used for horizon estimation are the same used in the attitude indicator included in aircraft cockpit instrumentation [16]. This procedure neglects topography variations within the operating area. For the sake of concreteness, it is useful to recall that in a stabilized North-East-Down (NED) reference frame with origin in the own-ship center of mass, assuming a spherical Earth with radius R_{Earth} and neglecting topography, horizon center is found at a negative elevation angle θ_0 given by

$$\theta_0 = -\cos^{-1}\left(\frac{R_{Earth}}{R_{Earth}+h}\right) \tag{1}$$

where h is the own-ship altitude. θ_0 increases in absolute value for increasing altitude, as shown in Figure 1. In general, an intruder aircraft will be found above the horizon if its elevation angle is larger than θ_0. θ_0 dependency on altitude also clarifies that the probability of a collision threat coming from below the horizon increases for decreasing flight altitude.

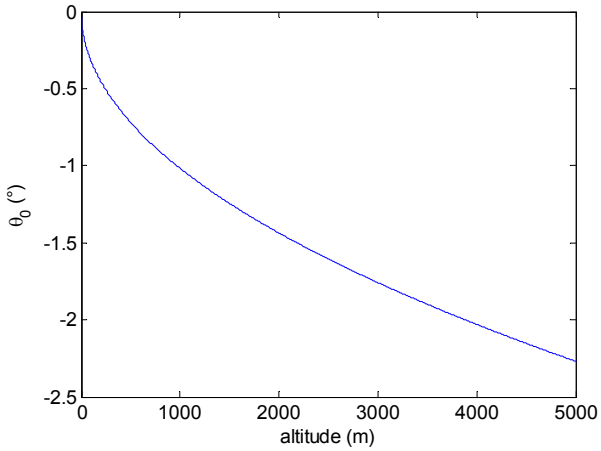

Figure 1. Elevation angle in NED coordinates for horizon center, as a function of own-ship altitude

Once the sky-region has been isolated, morphological filtering operations are carried out. Depending on weather and illuminations conditions, an intruder can appear as darker or brighter than the background. Thus, BH and TH filtering are both applied to the acquired images, using a 5 × 5 square structuring element. In fact, preliminary analyses showed a better performance of these filters compared with CMO processing, while eventual advantages that can be gained by more recent techniques such as ACBM are still under investigation. Indeed, even at long range with the aircraft imaged in a very few pixels, in some conditions there may be abrupt intensity changes within the aircraft shape (for example, between wing and fuselage), which is not consistent with the assumptions underlying these approaches. On the other hand, experimental results reported by other research groups [4] also did not show a significant performance increase by using ACBM in the framework of long range aircraft detection.

After morphological filters implementation, global thresholding is applied to remove image background and isolate regions of interest (ROI): pixels in the morphologically filtered images (sky region only) are selected if their intensity is above a threshold T_1 computed as

$$T_1 = \mu + k\sigma \tag{2}$$

where μ and σ refer to mean and standard deviation of pixel intensities, and k is a constant which can be tuned heuristically on the basis of flight data.

These ROI are not used directly as single frame detections within a multi-temporal processing stage. In fact, it is hard to find an acceptable trade-off between detection range and false alarm rate at this processing level: applying a relatively low threshold allows detecting the intruder at long range, but boundaries of small/dim clouds can create a significant number of false detections, which persist in subsequent images thus giving birth to false tracks.

Inspired by human-based detection, a further single frame criterion is thus applied which analyzes the areas (of the original, non filtered image) surrounding the ROI, as qualitatively shown in Figure 2. The basic concept is to estimate the homogeneity of these areas by computing the standard deviation of pixel intensities. Then, the criterion is based on computing the ratio between pixel intensities in the morphologically filtered image, and the standard deviation computed in the original image within the ROI neighborhood: if the ratio is not above a given threshold T_2, the corresponding ROI is discarded.

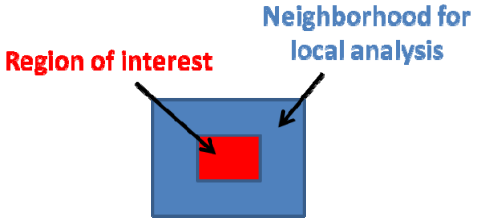

Figure 2. Qualitative view of region of interest and neighborhood for homogeneity evaluation

Again, T_2 can be tuned on the basis of flight data analysis. This processing allows eliminating both cloud boundaries which are detected by morphological operators (thanks to the relatively large standard deviation of local areas surrounding these pixels), and small very dim clouds (within the morphologically filtered image these pixels have a relatively small intensity, just above the global threshold).

After this local analysis, pixel centroiding is carried out to get the final single frame detections. It is useful to observe that in some cases the same aircraft can be detected both as a dark and a bright target, depending on the intensity features of the wing and the fuselage. Thus, centroiding is also used to fuse TH-based and BH-based detections. In order to enhance detection reliability especially at large ranges, centroiding is applied both to connected and almost connected pixels. Within this phase, a filter for saturated and almost saturated pixels is also applied to remove eventual direct or indirect effects of sun glares.

Single frame detections are provided as input to a multi-frame tentative tracking phase. In particular, based on navigation system outputs, tentative tracking is carried out in a stabilized NED reference frame. At this processing step, no intruder velocity estimation schemes are adopted, but a maximum possible angular rate in NED is considered to build gating areas and to associate subsequent morphological filtering (MF) based detections.

As an example, let us consider at time t_1 a single frame detection expressed in terms of pixel coordinates (x_1, y_1). First, the intrinsic camera model is used to estimate the unit vector $\hat{u}_1$ in the camera reference frame (CRF). The unit vector can be propagated to a subsequent frame acquired at a time instant t_2 using attitude measurements and camera alignment matrix as follows:

$$\hat{u}_2 = M_{CAM} M_{ATT2} M_{ATT1}^T M_{CAM}^T \hat{u}_1 \tag{3}$$

where M_{CAM} is the (constant) camera alignment matrix that converts from BRF to CRF, M_{ATT2} is the attitude matrix at time t_2, and M_{ATT1} is the attitude matrix at time t_1. Using again the intrinsic camera model, it is possible to calculate the predicted pixel coordinates at time t_2, i.e. (x_2, y_2).

A circular gate is now built around this prediction whose radius in pixels R_{max} can be related to the maximum angular rate in NED ω_{max} as follows:

$$R_{\max} \approx \frac{\omega_{\max}}{IFOV}\left(t_2 - t_1\right) \tag{4}$$

where IFOV is the camera instantaneous field of view. Thus, gate dimensions are basically controlled by the choice of ω_{max}. Within this framework, realistic values can be chosen considering the functional dependence of the distance at closest point of approach on angular rates [9] and making assumptions on range and range rate in the considered scenarios. It is worth noting that the developed technique is not aimed at detecting only collision course objects, which would not generate any dynamics in stabilized coordinates.

Once gates are generated, a classical measurement-to-track association procedure based on the nearest neighbor algorithm is implemented [17].

Track status is handled using the following modes:

- Single frame detections;
- Tentative tracks;
- Firm tracks. These represent confirmed detections to be provided to the high level tracking step and also to other functions such as collision detection and avoidance.

In particular, a tentative track is generated by associating two single frame MF-based detections in consecutive frames, while the transition tentative-firm is based on a 3-out-of-5 frames rule [17]. Three consecutive missed detections suffice for track deletion.

B. Target tracking: template matching and Kalman filtering

Once a confirmed detection is obtained, an obstacle template is generated, and the object is tracked in subsequent frames by using correlation-based algorithms [17]. In this "high-level" tracking phase, morphological filters are not used anymore for the confirmed tracks. Of course, within a multi-target perspective, morphological filters are still used for target detection in other areas of the camera FOV, outside search windows used for template matching.

Within this framework, Kalman filtering is used for optimal state estimation, in particular with the aim of estimating angular derivatives.

The problem of target tracking using passive sensors and no range information is widely discussed in literature [17]. In fact, own-ship maneuvers with an acceleration component that is perpendicular to the line of sight vector to the intruder are needed to estimate range and range rate, which are otherwise unobservable [18]. Standard tracking approaches such as linear dynamic models in Cartesian coordinates can have strong limitations in this framework, since they combine observable and unobservable states, so that the filter may become unstable before the range becomes observable due to own-ship accelerations. More efficient techniques such as modified spherical coordinates (MSC [19]) are able to keep stability in these cases, paying the cost of an increase in complexity and computational burden.

In fact, in collision avoidance scenarios range observability is not always ensured, mainly because of short time to collision and limited aircraft maneuverability. On the other hand, electro-optical sensors usually exhibit large frame rates (of the order of 10 Hz or more) and fine angular accuracy, so that even using azimuth and elevation angles (and their rates) as states, target pseudo-accelerations due to problem non linearities and/or maneuvers are bounded, apart from the case of very small ranges. Thus, a simplified filtering approach has been used, with two independent two-state linear Kalman filters for azimuth and elevation angles in NED, both based on nearly constant velocity models [17].

Considering for example the azimuth angle φ, the state vector is defined as

$$x = \begin{bmatrix} \varphi \\ \dot{\varphi} \end{bmatrix} \tag{5}$$

and the dynamic model in discrete terms is given by

$$x(k+1) = \Phi x(k) + v(k) \tag{6}$$

$$\Phi = \begin{bmatrix} 1 & T \\ 0 & 1 \end{bmatrix} \tag{7}$$

where T is the sampling time taken as the inverse of camera frame rate, and the process noise matrix Q is evaluated as

$$Q = E\left[v(k)v(k)^T\right] = q_\varphi \begin{bmatrix} \frac{T^3}{3} & \frac{T^2}{2} \\ \frac{T^2}{2} & T \end{bmatrix} \tag{8}$$

The scale factor q_φ is related to the azimuth rate change over a sampling interval. Thus, it allows process noise matrix to be dimensioned considering worst case angular accelerations that can be realistically found in the considered case.

The measurement equation is linear and is given by

$$y(k) = Hx(k) + w(k) \tag{9}$$

where

$$H = \begin{bmatrix} 1 & 0 \end{bmatrix} \tag{10}$$

while the measurement covariance matrix $R = E\left[w(k)w(k)^T\right]$ reduces to a single scalar quantity σ_φ^2 that includes both camera resolution and attitude measurement noise.

A similar filter is used for the elevation in NED, while image windows for correlation-based matching are built with some margins, to reduce the risk of track loss.

In spite of the simplicity and theoretical limitations of this approach (which does not explicitly include own-ship accelerations in the state estimation process), it has demonstrated to be reliable and accurate for the problem under analysis, as it will be shown in the following.

A complete flow diagram of the detection and tracking algorithm is depicted in Figure 3.

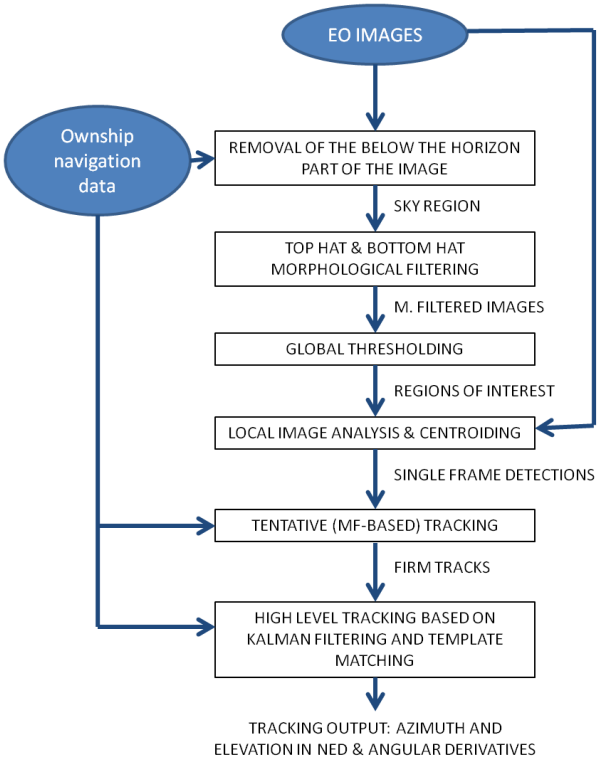

Figure 3. Flow diagram of the vision-based detection and tracking algorithm

This global view of the algorithm clarifies that its originality lies in the customized combination of different techniques. However, it is also useful to underline novel implementation aspects relevant to the single blocks, such as:

- TH and BH filters are not used independently: TH-based and BH-based detections are fused together;

- target centroiding includes almost connected pixels too;

- local image analysis is used to combine at pixel level morphologically filtered and unfiltered images;

- multi-frame processing is aimed not only at detecting collision course objects, but all the intruders whose angular rates are below assumed limits.

C. Algorithm tuning strategy

Algorithm performance is closely related to a proper choice of tuning parameters. Some of these parameters, such as R_{max} or q_{φ}, depend on the considered assumptions on relative dynamics. As in most tracking applications, they result from a compromise between contradicting requirements such as tracking accuracy and risk of track loss.

Other tuning parameters, such as k and T_2, are relevant to the image-based obstacle detection process. In this case, due to the variability and complexity of illumination and visibility conditions, a theoretical approach is hard to be implemented. Instead, an experimental approach based on images gathered in flight is preferred to focus the performance impact of different parameter choices. Of course, in this case it is important to have a large experimental data set covering different conditions.

This analysis has been conducted at a preliminary level considering a subset of experimental conditions, which led to the tuning parameters used in the simulations described in the following. Performance analysis on the whole TECVOL data base, including electro-optical images and navigation system measurements relevant to chasing flight and near collision encounters, is under way and results will be published in future works. However, it is useful to clarify the adopted processing strategy:

- GPS data are used to evaluate "true" relative position and velocity;

- estimated relative dynamics allows flight segments of interest to be extracted;

- for any given combination of tuning parameters, the detection and tracking algorithm is run on the selected flight segments;

- system output statistics are computed. In particular, comparison of reference (GPS-based) azimuth and elevation and firm tracks estimates is used to individuate true/false tracks;

- a supervised analysis is adopted to confirm processing results.

This strategy allows deriving performance statistics such as detection range and false alarm rate for any given combination of tuning parameters. Thus, on one hand an optimal parameter combination can be selected which gives a reliable performance in highly variable conditions. On the other hand, the possible implementation of an adaptive algorithm can be analyzed, where image processing parameters are controlled in real time based on the operating conditions. However, a possible limitation of an adaptive approach lies in the inherent local nature of target detectability, which is not well characterized by global image statistics [4].

III. Experimental Results

A. Overview of flight setup and testing architecture

As anticipated above, performance of vision-based detection and tracking can be estimated using flight data gathered during tests relevant to multi-sensor-based collision detection and avoidance. For the sake of clarity, a brief overview of flight system setup and testing architecture is presented here, while the reader is referred to Refs. 7 and 9-12 for a detailed description of architectures and algorithms implemented in flight.

The test platform is an optionally piloted laboratory aircraft of ultra light category named FLARE (Flying Laboratory for Aeronautical REsearch), which is a customized TECNAM P-92. It is equipped with different non cooperative sensors (35 GHz radar, infrared and daylight optical cameras), as shown in Figure 4.

Figure 4. FLARE with radar/optical sensors installed on top of the wing

Within the sensing system, a forward looking panchromatic camera is considered in this paper as the basic sensor for standalone EO detection and tracking. It is a commercial-off-the-shelf (COTS) camera with a FOV of approximately 52.9° x 40.8°, while the IFOV is of the order of 0.040°. The considered camera FOV does not satisfy general sense and avoid requirements [9] but suffices for a technology demonstration in quasi frontal near collision geometries.

In terms of navigation sensors, the aircraft is equipped with a laser altimeter, GPS antennas and receivers, an Air Data Sensor, and a COTS Attitude and Heading Reference System (AHRS) including magnetometers and MEMS-based accelerometers and gyroscopes.

In order to ensure execution of collision avoidance flight tests, a dedicated system has been developed with a ground control station dedicated to experiments monitoring and control. Flight tests relevant to obstacle detection and tracking, and autonomous non cooperative collision avoidance, are carried out using as intruder a piloted ultra-light aircraft, equipped with a GPS receiver, a processing unit to store flight test data, and a RF transmitter to download position data to the ground station. In fact, correct and safe execution of flight tests requires that the intruder is properly synchronized with FLARE in order to realize the desired approaching geometries. Within this framework, ground station software is used by flight test engineers to monitor test status especially regarding relative position and velocity, and to send commands to the flight system.

Some flight tests are carried out with FLARE aircraft piloted by the safety pilot, while other tests are executed with FLARE flying in autonomous mode. Of course, the latter mode in the one adopted in autonomous collision avoidance tests. Two basic types of maneuvers have been tested:

1. Tail chase tests with FLARE pursuing the intruder. These tests allow gathering a large quantity of sensor data with smooth relative dynamics.

2. Frontal and near-frontal encounters. In all these tests, which are the most important from the application point of view, slight altitude differences are commanded between aircraft for safety reasons, with the intruder at higher altitude than FLARE in most cases. It is worth noting that the reliability of flight monitoring systems, the adoption of ultra-light aircraft as test platforms, and the skills of test pilots allow generating realistic collision geometries, with small distances at closest point of approach and a significant amount of useful radar and optical data.

B. *Performance evaluation*

Detection and tracking performance evaluation is carried out considering two near collision encounters in different flight tests. While local time and thus theoretical illumination conditions are similar (sun is in the back of the camera), the difference in weather and visibility heavily impacts the operating environment in terms of background homogeneity and intruder appearance.

Test case 1 is characterized by good visibility conditions, with a significant intruder contrast with respect to the background even at relatively large range. However, background is largely non homogeneous because of a significant number of small white clouds. Most of these clouds are found near the horizon, close to the intruder aircraft. Moreover, both intruder and clouds are brighter than the background. This scenario is thus challenging especially in terms of robustness to false detections. An example image comprising the intruder aircraft at a range of about 1.3 km is shown in Figure 5.

Test case 2 is relevant to an encounter experimented in hazy conditions and worse visibility than the previous case. Background is largely homogeneous especially near the horizon, while the mean intensity changes completely at high elevation angles because of sun illumination effects. While the intruder is still brighter than its local background, for a given range the contrast is greatly reduced with respect to the previous case. It can be concluded that this scenario is challenging especially from the detection range point of view. As before, an example image with the intruder aircraft at a range of about 1.3 km is shown in Figure 6.

In the considered flight tests, EO data were acquired at 3.3 Hz due to limitations on the mass memory of the on board computer. Thus, images are processed at this frequency. In both test cases, the analysis focuses on flight segments at a range larger than 1.3 km, since the major interest is in understanding algorithm potential for relatively large time to collision, when the intruder spans a very few pixels but at the same time effective collision detection can enable safe avoidance maneuvers. At lower ranges increased contrast and number of intruder pixels make the detection and tracking problem of easier solution.

The same algorithm tuning parameters are adopted in the two test cases. Regarding detection parameters, both k and T_2 are set equal to 6.

Considering test case 1, detection and tracking results are depicted in Figure 7, which reports GPS-based estimates (reference measurements), and azimuth and elevation in NED relevant to single frame detections, tentative tracks, and firm tracks. In particular, in the firm tracking phase both template matching-based detections and filtered outputs are presented. While a significant number of single frame detections is found, their random nature in time allows effective filtering by multi-frame processing techniques adopted for tentative tracking: single frame detections due to false targets do not associate in subsequent frames, and no false tracks are produced. Single frame detections are

distributed almost symmetrically within the azimuth FOV, while elevation measurements are usually found at larger angles than the intruder which is due to the fact that it flies close to the horizon and the analysis is applied to the sky region of the image.

A single tentative and then firm track is generated which corresponds to the real intruder. Mainly due to the visibility conditions, range at firm tracking is large: about 2.6 km. No track losses are experimented, and the tracking algorithm reliably estimates intruder motion during the whole considered flight segment. Elevation estimates are with good approximations unbiased, while azimuth detections and filtered estimates exhibit a bias of the order of 2° mostly due to a similar bias in magnetic heading estimation by the commercial AHRS installed onboard, which affects measurement conversion in NED. The bias can be better appreciated in Figure 8 which depicts angular errors during firm tracking. Both in azimuth and in elevation, the implemented Kalman filter is able to filter out some measurement noise. In spite of the equal camera azimuth and elevation IFOV, a slightly larger error noise is found in azimuth, which is again mostly due to magnetic heading measurement noise. Standard deviation of angular errors in NED is of the order of less than 0.3° in azimuth, and about 0.1° in elevation. It is worth underlining that error magnification with respect to camera IFOV is mostly due to AHRS effects. Figure 9 and Figure 10 show angular rate estimation capabilities of the implemented algorithms. As a result of null or almost constant angular error biases, both azimuth rate and elevation rate estimates are with good approximation unbiased, while the error standard deviation is found to be of the order of 0.1 °/s for the azimuth rate and 0.04 °/s for the elevation rate.

In order to show the effectiveness of the combination of morphological filtering and local image analysis, it is useful to have a look at the output of the detector based on morphological filtering when the local analysis of regions of interest is not implemented.

A typical result is shown in Figure 11, where it can be seen how small and dim clouds generate a significant number of false single frame detections, which cannot be removed by multi-frame processing as they are found in several subsequent frames. As a result, a significant number of false tracks (6 in the considered encounter) is generated in a few frames. In order to remove these detections, a larger global threshold should be applied to the whole morphologically filtered image, paying the cost of a reduction of intruder detection range.

Detection and tracking performance in test case 2 shows similarities and differences. As done for the first test case, GPS-based estimates and algorithm outputs in terms of azimuth and elevation in NED are depicted in Figure 12. A single tentative and then firm track is generated which corresponds to the real intruder, but the mean number of single frame detections is much smaller than before. Range at firm tracking is also lowered by weather conditions and the reduced intruder contrast, and is found to be of about 1900 m. As before azimuth errors are affected by an almost constant bias, which differs in sign from test case 1 though being of the same order of magnitude. More importantly, angular rate estimates are unbiased and their dynamics and errors are very similar to test case 1.

For the sake of brevity, error diagrams for test case 2 are not reported. Instead, Table I quantitatively summarizes algorithm performance in the two considered test cases.

Computed error statistics (mean, standard deviation, and root mean square error) and performance parameters confirm algorithm robustness in spite of completely different operating conditions. In summary, as it could be expected detection range is affected by visibility conditions, but even in the most challenging scenario range at firm tracking is only slightly smaller than 2 km (and corresponds to a time to collision of about 22 s, considering the closing speed). On the other hand, in both test cases no false tracks are generated, and tracking accuracy is of the same order of magnitude. In particular, angular rate error mostly falls below 0.1 °/s. This does not represent the best performance that could be achieved by the considered camera and frame rate, mainly because of the degradation induced by AHRS attitude measurement noise.

Recent flight tests have been carried out with a new AHRS based on latest generation MEMS sensors and an enhanced auto-calibration procedure. These flight data are under analysis and will be discussed in future works.

In any case, it is worth underlining that the performance in terms of detection range (at firm tracking) and false alarm rate seems promising with respect to similar research experiences, especially if the relatively large camera IFOV is taken into account. Of course, performance evaluation on a larger experimental data set is needed to increase the statistical significance of these results.

TABLE I. PERFORMANCE SUMMARY IN THE CONSIDERED TEST CASES

Performance indexes		**Test case 1**	**Test case 2**
Azimuth error in NED (°)	***Mean***	-2.0	2.4
	Std	0.26	0.26
	Rms	2.0	2.5
Elevation error in NED (°)	***Mean***	-0.079	0.055
	Std	0.12	0.21
	Rms	0.14	0.21
Azimuth rate error in NED (°/s)	***Mean***	-0.0016	0.022
	Std	0.11	0.13
	Rms	0.11	0.13
Elevation rate error in NED (°/s)	***Mean***	-0.014	-0.049
	Std	0.043	0.10
	Rms	0.045	0.11
Range at firm tracking (m)		2622	1836
Mean number of single frame detections		0.54	0.19
Number of false tracks		0	0

Figure 5. Image from test case 1. The red arrow points to the intruder aircraft at a range of about 1.3 km

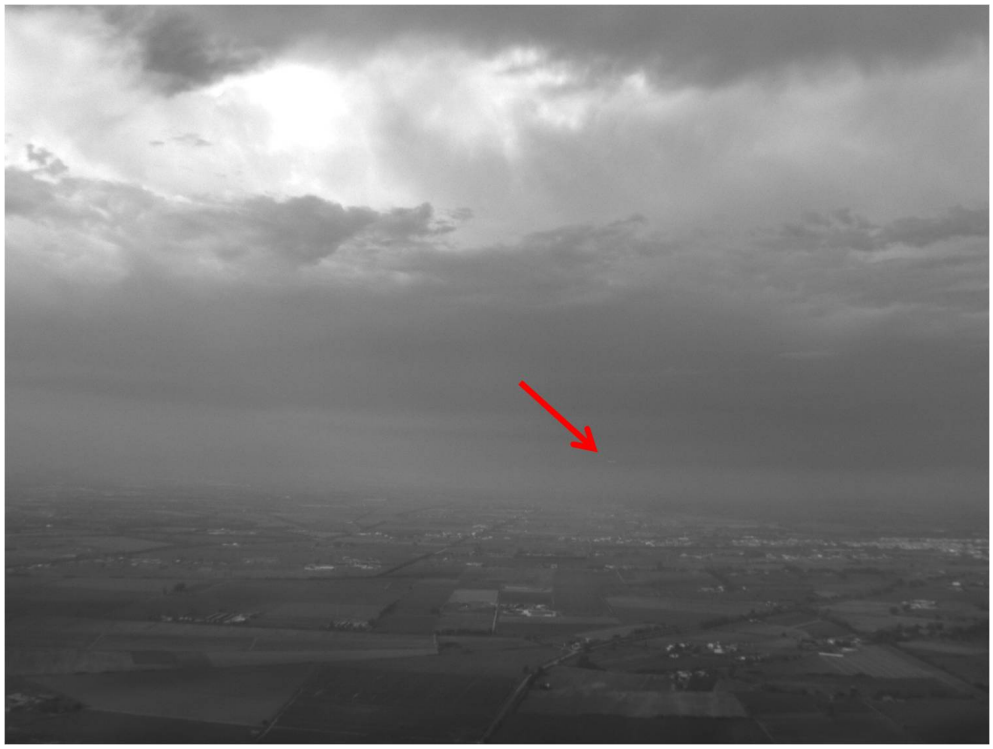

Figure 6. Image from test case 2. The red arrow points to the intruder aircraft at a range of about 1.3 km

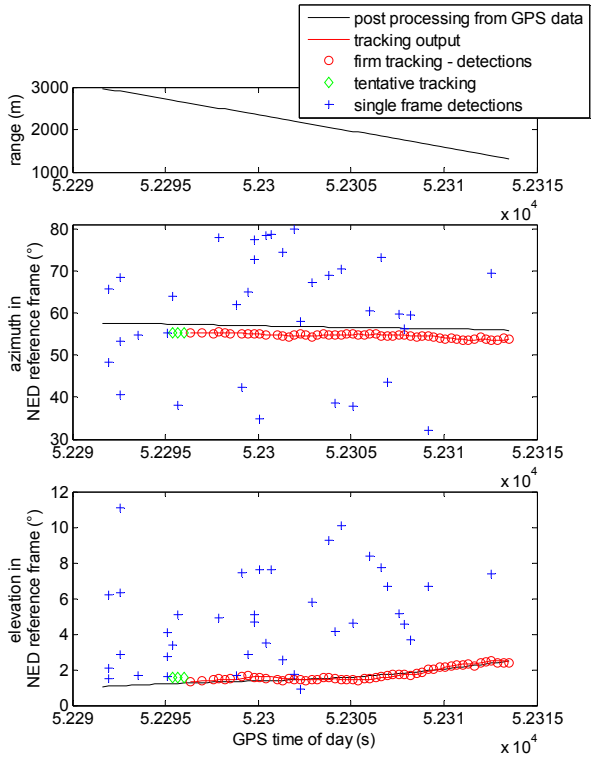

Figure 7. Range and angles in test case 1, as a function of GPS time of day. GPS position measurements are used as reference

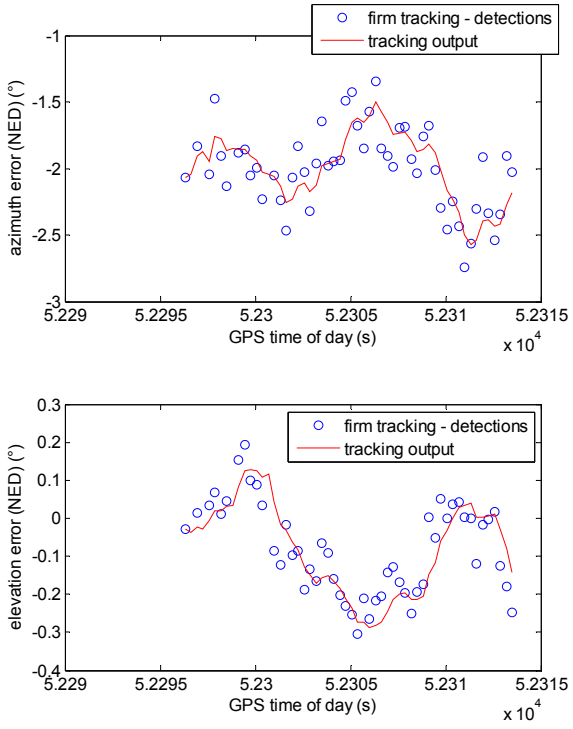

Figure 8. Azimuth and elevation errors in test case 1 (firm tracking only) as a function of GPS time of day

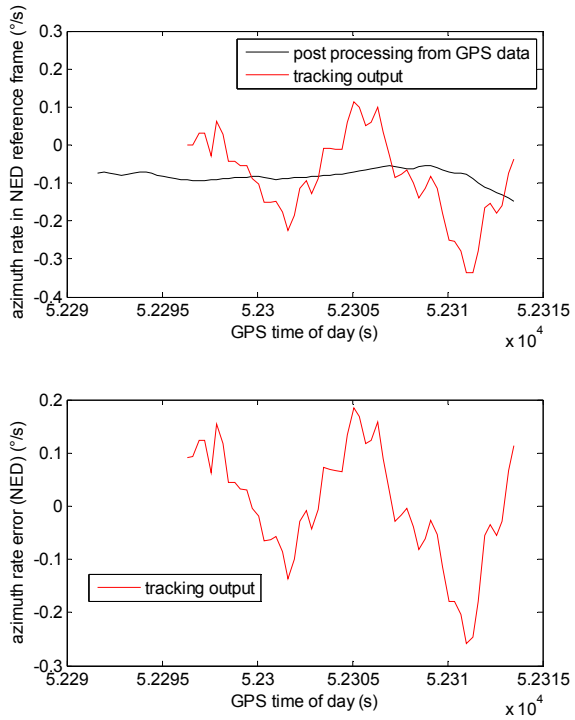

Figure 9. Azimuth rate (GPS and tracker), and error w.r.t. GPS (tracker) as a function of time in test case 1

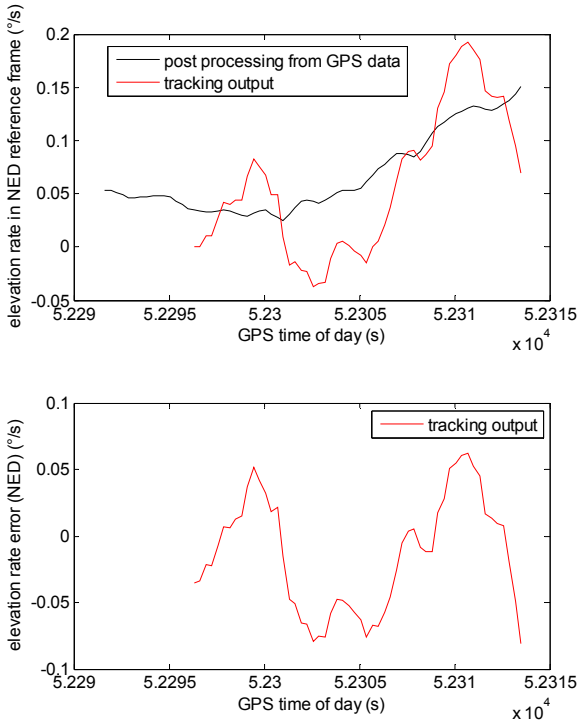

Figure 10. Elevation rate (GPS and tracker) and error w.r.t. GPS (tracker) as a function of time in test case 1

Figure 11. Single frame detections obtained using morphological filtering and global thresholding, without local analysis of regions of interest (test case 1)

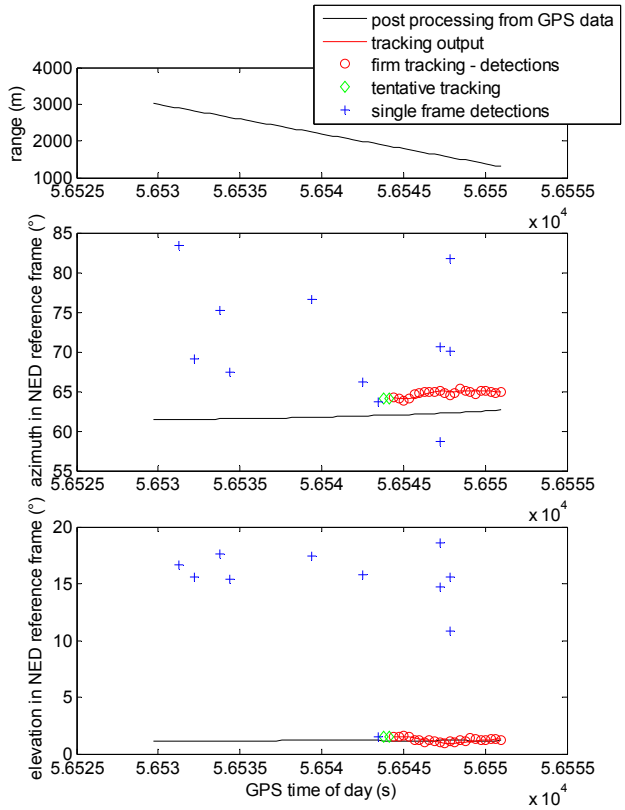

Figure 12. Range and angles in test case 2, as a function of GPS time of day. GPS position measurements are used as reference

IV. Conclusion

This paper focused on a detection and tracking algorithm for vision-based sense and avoid. It combines electro-optical images and navigation system measurements and it comprises two main steps. The first processing step is aimed at obstacle detection and tentative tracking, and is based on morphological filtering, local image analysis, and multi-frame processing in stabilized coordinates. The second processing step is activated for firm tracks and is based on template matching and a conventional Kalman filtering-based state estimation algorithm. Performance analysis on flight data gathered in realistic near collision scenarios showed a detection range of the order of 2 km, reliable filtering of false positives with no false tracks, accurate angular and angular rate estimates (errors on azimuth rate and elevation rate estimates mostly below 0.1 °/s), and a limited sensitivity on weather and illumination conditions.

Current research activities are aimed at evaluating performance in a wide set of experimental conditions including different navigation system options, also in view of a quantitative analysis of the trade-off between detection range and false alarm rate.

REFERENCES

[1] Federal Aviation Administration, "Integration of Civil Unmanned Aircraft Systems (UAS) in the National Airspace System (NAS) Roadmap", First Edition - 2013.

[2] B. Stark, B. Stevenson, and C. YangQuan, "ADS-B for small Unmanned Aerial Systems: Case study and regulatory practices", *International Conference on Unmanned Aircraft Systems (ICUAS) 2013*, Atlanta, GA, 28-31 May 2013, pp.152-159.

[3] J. Utt, J. McCalmont, and M. Deschenes, "Development of a Sense and Avoid System", *AIAA Infotech@Aerospace Conference 2005*, Arlington, VA, Sep. 26-29, 2005, pp- 1-10 .

[4] J. Lai, J.J. Ford, L. Mejias, and P. O'Shea, "Characterization of Sky-region Morphological-temporal Airborne Collision Detection", *Journal of Field Robotics*, Volume 30, Issue 2, pages 171–193, March/April 2013.

[5] D. Dey, C.M. Geyer, S. Singh, and M. Digioia, "A cascaded method to detect aircraft in video imagery", *The International Journal of Robotics Research*, Vol. 30, No. 12, October, 2011, pp. 1527 - 1540.

[6] B. Vanek, T. Péni, A. Zarándyx, J. Bokor,T. Zsedrovitsk, and T. Roska, "Performance Characteristics of a Complete Vision Only Sense and Avoid System", *AIAA Guidance, Navigation, and Control Conference 2012*, Minneapolis, MN, 13 - 16 August 2012, AIAA paper 2012-4703.

[7] G. Fasano, D. Accardo, A. Moccia, C. Carbone, U. Ciniglio, F. Corraro, and S. Luongo, "Multi-Sensor-Based Fully Autonomous Non-Cooperative Collision Avoidance System for Unmanned Air Vehicles," *AIAA Journal of Aerospace Computing, Information, and Communication*, vol. 5, pp. 338-360, October 2008.

[8] R.H. Chen, A. Gevorkian, A. Fung, and W.Z. Chen, "Multi-Sensor Data Integration for Autonomous Sense and Avoid", *AIAA Infotech@Aerospace Technical Conference 2011*, St. Louis, Missouri

[9] D. Accardo, G. Fasano, L. Forlenza, A. Moccia, and A. Rispoli, "Flight Test of a Radar-Based Tracking System for UAS Sense and Avoid", *IEEE Transactions on Aerospace and Electronic Systems*, vol.49, no.2, pp.1139,1160, April 2013

[10] G. Fasano, L. Forlenza, D. Accardo, A. Moccia, A. Rispoli, "Integrated Obstacle Detection System based on Radar and Optical Sensors", *AIAA Infotech@Aerospace 2010*. Atlanta GA, 20-22 April 2010, Paper AIAA 2010-3421

[11] S. Luongo, V. Di Vito, G. Fasano, D. Accardo, L. Forlenza, and A. Moccia, "Automatic Collision Avoidance System: Design, Development and Flight Tests", *30th IEEE/AIAA Digital Avionics Systems Conference*, Seattle WA 2011.

[12] G. Fasano, D. Accardo, A.E. Tirri, A. Moccia, and E. De Lellis, "Flight Performance Assessment of Vision-based Detection and Tracking for UAS Sense and Avoid", *Infotech@Aerospace Conference 2013*, Boston MA, August 2013.

[13] R.C. Gonzalez and R.E. Woods, *Digital Image Processing, Third Edition*, Prentice Hall (Pearson International Edition)

[14] X. Bai, F. Zhou, Y. Xie, and T. Jin, "Enhanced detectability of point target using adaptive morphological clutter elimination by importing the properties of the target region", *Signal Processing*, 89(10), pp. 1973–1989, 2009

[15] G. Fasano, D. Accardo, A. Moccia, and A. Rispoli, "An Innovative Procedure for Calibration of Strapdown Electro-Optical Sensors Onboard Unmanned Air Vehicles", *Sensors*, Vol. 10, No. 1, pp. 639-654, 2010.

[16] R. P. G. Collinson, *Introduction to Avionics*, vol. 11 of Microwave Technology Series, Chapman&Hall, 1996

[17] S.S. Blackman and R.F. Popoli, *Design and Analysis of Modern Tracking Systems*, Artech House, Norwood MA, 1999, pp. 360-372

[18] O. Shakernia, W.-Z. Chen and V.M. Raska, "Passive Ranging for UAV Sense and Avoid Applications", *AIAA Infotech@Aerospace 2005*, 26-29 September 2005, paper AIAA 2005-7179,

[19] D.V. Stallard, "Angle-Only Tracking Filter in Modified Spherical Coordinates", *Journal of Guidance, Control and Dynamics*, Vol. 14, N. 3, pp. 694-696, May-June 1991.